Hole initiated impact ionization in wide band gap semiconductors

Martin Reigrotzki, Ronald Redmer, and Niels Fitzer
Fachbereich Physik, Universität Rostock, Universitätsplatz 3, D-18051 Rostock, Germany

Stephen M. Goodnick and Manfred Dür[a)]
Department of Electrical Engineering, Arizona State University, Tempe, Arizona 85287-5706

Wolfgang Schattke
Institut für Theoretische Physik, Christian-Albrechts-Universität Kiel, Leibnizstrasse 15, D-24118 Kiel, Germany

(Received 15 March 1999; accepted for publication 1 July 1999)

Band-to-band impact ionization by hot electrons and holes is an important process in high-field transport in semiconductors, leading to carrier multiplication and avalanche breakdown. Here we perform first principles calculations for the respective microscopic scattering rates of both electrons and holes in various wide band gap semiconductors. The impact ionization rates themselves are calculated directly from the electronic band structure derived from empirical pseudopotential calculations for cubic GaN, ZnS, and SrS. In comparison with the electron rates, a cutoff in the hole rate is found due to the relatively narrow valence bandwidths in these wide band gap semiconductors, which correspondingly reduces hole initiated carrier multiplication. © *1999 American Institute of Physics.* [S0021-8979(99)08419-4]

I. INTRODUCTION

Charge transport in semiconductors at low electric fields can be described within linear response theory considering elastic electron–electron and electron–impurity scattering as well as inelastic electron–phonon scattering processes. For higher fields, in the MV/cm range, optical phonon scattering and band-to-band impact ionization may become the dominant scattering mechanisms for the thermalization of the charge carriers. In particular, the high-field distribution of hot electrons in thin-film electroluminescent (TFEL) devices is critical in determining the impact excitation rate of luminescent centers in wide band gap phosphors such as ZnS and SrS. Carrier multiplication plays a significant role in the TFEL device performance, including such effects as field clamping.[1,2]

The *ab initio* calculation of the respective microscopic scattering rates for semiconductor materials under the influence of high electric fields is still an open problem. First, a realistic band structure has to be taken into account. Second, the treatment of high-field effects, such as the intracollisional field effect and collision broadening, requires an adequate quantum transport theory. Third, the physical quantities are given by high-dimensional integrals over the entire Brillouin zone, the evaluation of which requires the application of special numerical methods. Finally, the coupled transport of electrons and holes in the actual semiconductor material has to be described within a self-consistent framework such as full-band Monte Carlo simulation methods or a direct solution of the quantum kinetic equation.

For practical applications, the microscopic impact ionization process is of special interest. It is related to the macroscopic ionization coefficient α, which is experimentally accessible by measuring the carrier multiplication factor. However, assumptions about the microscopic impact ionization rates have to be made. In many cases, the hole initiated impact ionization rate is supposed to be equal to the electron rate, which has to be verified for the semiconductor material under consideration.

We have previously calculated the electron initiated, wave vector dependent impact ionization rate for Si, GaAs,[3] ZnS,[4–6] and GaN.[7] The respective energy dependent impact ionization rates have already been used in full-band Monte Carlo simulations of high-field electron transport.[5–7] Based on that microscopic approach, we present new results for the hole initiated impact ionization rates for the cubic wide band gap materials ZnS, GaN, and SrS, which show a very different behavior than the electron rates. These new results are important for the interpretation of the measured impact ionization coefficient. For example, assuming that the electron and hole rates are almost identical, the impact ionization coefficient at high fields was extracted from experimental carrier multiplication data for ZnS.[8] We show that this equality is not expected to be valid based on the present numerical results for the electron and hole rates, and we rederive the experimental impact ionization coefficient for ZnS assuming only electrons.

II. IMPACT IONIZATION OF ELECTRONS

A. Impact ionization rate

The ionization rate of valence band electrons due to scattering by conduction band electrons is usually determined from Fermi's golden rule as

a)Electronic mail: duer@asu.edu

 © 1999 American Institute of Physics

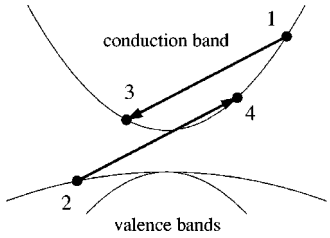

FIG. 1. Schematic impact ionization process for electrons (process I).

$$r(\mathbf{k}_1,n_1)=\frac{2\pi}{\hbar}\frac{V^3}{(2\pi)^9}\sum_{n_2,n_3,n_4}\int\int\int d^3\mathbf{k}_2\,d^3\mathbf{k}_3\,d^3\mathbf{k}_4 \times|M_{\mathrm{tot}}(1,2;3,4)|^2\delta[E_{n_1}(\mathbf{k}_1)+E_{n_2}(\mathbf{k}_2) -E_{n_3}(\mathbf{k}_3)-E_{n_4}(\mathbf{k}_4)], \quad (1)$$

where V is the crystal volume, and $\mathbf{k}_i$ and n_i are the wave vector and the band index, respectively, labeling Bloch electron state $i\in\{1,2,3,4\}$ with energy $E_{n_i}(\mathbf{k}_i)$. M_{tot} denotes the matrix element for impact ionization including direct, exchange, and umklapp processes. Here, the initial electron states $i=1,2$ correspond to an electron in the conduction band and a second electron in the valence band. The final states $i=3,4$ are for both electrons in the conduction band, as illustrated in Fig. 1.

The integrals in Eq. (1) extend over the entire Brillouin zone and are evaluated using an efficient numerical procedure developed by Sano and Yoshii.[9] Making extensive use of symmetry relations imposed by the crystal structure, the integrations can be restricted to the irreducible wedge of the Brillouin zone where a large number of points can be taken into account for the numerical evaluation. We use a uniform grid in wave vector space with 152 points in the irreducible wedge corresponding to 4481 points across the whole Brillouin zone. Although the error introduced by discretization is most pronounced in the threshold region, previous calculations[3–6] have shown that the chosen grid spacing leads to fairly accurate results for the impact ionization rate in this region. A further increase of the number of grid points does not affect the calculated rate significantly. The interaction between the conduction and valence electrons is described by a wave vector dependent dielectric function derived by Levine and Louie.[10] The frequency dependence of the dielectric function becomes more important as the energy of charge carriers increases. At high energies, we observe that primarily umklapp processes (which we take into account up to the sixth order) contribute to the calculated rate and, therefore, due to the large momentum transfer, the influence of the carrier energy on the screening function is less important. Jung *et al.*[11] have employed a wave vector and frequency dependent dielectric function within the random-phase approximation for the calculation of the impact ionization rate in GaAs using a Monte Carlo integration technique. Their results agree well with our findings, which were obtained using a static dielectric function.[3] Nevertheless, the use of a wave vector and frequency dependent dielectric function would be more appropriate and should be considered in forthcoming studies.

TABLE I. Fourier coefficients of the pseudopotential parameters (in eV). The reciprocal lattice vectors G are given in units of $(2\pi/a)$.

Coefficient	GaN			
$V(\mathrm{G})$	A[a]	B[b]	ZnS[c]	SrS[d]
$V_S(\sqrt{3})$	−4.082	−4.354	−2.966	⋯
$V_S(\sqrt{4})$	⋯	⋯	⋯	−2.655
$V_S(\sqrt{8})$	0.816	0.408	0.626	0.264
$V_S(\sqrt{11})$	0.952	0.816	0.980	⋯
$V_S(\sqrt{12})$	⋯	⋯	⋯	−0.681
$V_A(\sqrt{3})$	3.810	3.401	2.463	3.274
$V_A(\sqrt{4})$	2.721	2.857	1.415	0.0
$V_A(\sqrt{11})$	0.544	0.272	0.204	−0.267
$V_A(\sqrt{12})$	0.272	0.0	0.204	0.0

[a]Provided by P. Vogl, Walter Schottky Institute, Munich.
[b]From Ref. 14.
[c]With nonlocal corrections: Gaussian potential with $R_2^{\mathrm{Zn}}=R_2^{\mathrm{S}}=1.22$ Å, $A_2^{\mathrm{Zn}}=-1.70$ eV, $A_2^{\mathrm{S}}=6.87$ eV.
[d]With nonlocal corrections: Gaussian potential with $R_2^{\mathrm{Sr}}=1.89$ Å, $A_2^{\mathrm{Sr}}=-8.932$ eV. Due to the slightly different crystal structure, $V_S(\sqrt{3})$ and $V_S(\sqrt{11})$ are replaced by $V_S(\sqrt{4})$ and $V_S(\sqrt{12})$. Parameters provided partly by P. Vogl, Walter Schottky Institute, Munich.

The wave vector dependent impact ionization rate $r(\mathbf{k}_1,n_1)$ is averaged over the entire Brillouin zone to obtain an energy dependent rate $R(E)$ according to

$$R(E)=\frac{\sum_n\int d^3k\;\delta[E-E_n(\mathbf{k})]r(\mathbf{k},n)}{\sum_n\int d^3k\;\delta[E-E_n(\mathbf{k})]}, \quad (2)$$

where n runs over all conduction bands. Equation (2) is well fit by a power law relation of the form

$$\tilde{R}(E)=P[E-E_{\mathrm{th}}]^a. \quad (3)$$

The energy dependent electron impact ionization rate according to Eq. (3) can be included in full-band Monte Carlo simulations of electronic transport in semiconductors.

B. Band structure

The electronic band structure of the semiconductor is the basic input to evaluate Eq. (1) numerically. We apply the empirical pseudopotential method (EPM),[3,12] which represents a compromise between the required accuracy and the available computer resources. In this method, the Bloch functions are expanded in terms of a plane wave basis. The matrix elements of the crystal potential are treated as adjustable parameters which are fit to experimental data such as gap energies. In a local EPM calculation, the dependence of the pseudopotential on the angular momentum components present in the atomic core states is ignored. Nonlocal correction terms may be added to account for this dependence. A fixed set of 113 reciprocal lattice vectors was used throughout this paper for ZnS, GaN, and SrS. The symmetric and antisymmetric pseudopotential parameters are listed in Table I. For GaN, the calculations were performed using the local EPM parameter set A. In order to compare with previous results for the

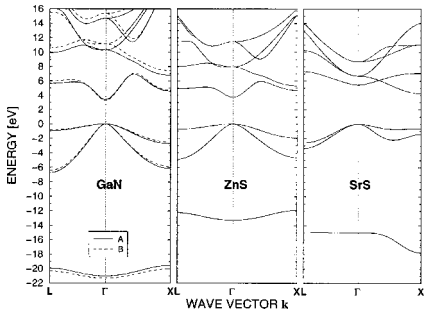

FIG. 2. EPM band structures of cubic GaN, ZnS, and SrS used in the present calculations. The GaN band structure is calculated using two different parameter sets *A* and *B*.

hole initiated impact ionization rate,[13] the underlying band structure *B* proposed by Oguzman *et al.*[14] was also employed in our calculations. For ZnS, the nonlocal pseudopotential parameters from our previous calculation of the electron initiated impact ionization rate[5] were used. In the case of SrS, the EPM band structure is not well understood, since relatively little experimental data exists for this material. The present band structure was obtained by fitting the critical point energies reported by Kaneko and Koda.[15] Comparison with recent band structure calculations based on an extended local density approximation including an exact exchange term[16] suggests that our calculation should give qualitatively correct results.

Figure 2 shows the respective EPM band structures. Special transition energies are listed in Table II. Both zincblende GaN and ZnS are direct band gap materials, whereas SrS (rocksalt) is indirect. Apart from the fundamental gap between the valence and the conduction bands, a second gap within the valence bands occurs. This second gap separates the lowest from the upper three valence bands and results in a forbidden energy region in the hole energy spectrum.

C. Results for the impact ionization rate

The wave vector dependent, electron initiated impact ionization rates have been calculated for the wide band gap materials ZnS,[4–6] GaN,[7,17] and SrS according to Eq. (1) using the EPM band structures given in Fig. 2 and taking into account umklapp processes up to the sixth order.[3] We show

TABLE II. Transition energies associated with the calculated EPM band structures (in eV). Indices denote the lowest conduction band (c) and the highest valence band (v) at the respective points. The fundamental gap is typed in boldface. Note that SrS shows an indirect fundamental gap. The gap between the lowest and the upper valence bands (vb gap) which is important for the hole impact ionization rates is also given.

	GaN			
Transition	*A*	*B*	ZnS	SrS
$\Gamma_v-\Gamma_c$	**3.39**	**3.28**	**3.73**	5.45
L_v-L_c	6.57	6.84	5.60	9.92
X_v-X_c	7.28	7.17	6.58	4.86
Γ_v-X_c	4.58	4.70	4.69	**4.26**
Γ_v-L_c	5.63	6.01	4.89	7.35
vb gap	12.82	13.56	7.04	11.51

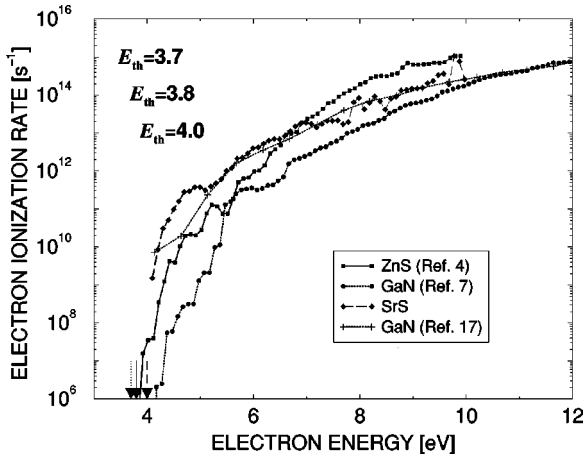

FIG. 3. Energy dependent electron impact ionization rate for the wide band gap materials ZnS, GaN, and SrS. The arrows mark the threshold energies.

the corresponding energy dependent impact ionization rates, Eq. (2), in Fig. 3 in order to compare later with the behavior of the respective hole rates. The parameters of the fit formula, Eq. (3), are given in Table III.

III. IMPACT IONIZATION OF HOLES

A second possible electron–electron scattering process of the same order may take place by the relaxation of a valence band electron, passing enough energy to a second valence band electron to be ionized across the gap into the conduction band and generate an additional free carrier.

This scattering process can be understood as the scattering of two holes in which a hole residing in the conduction band is ionized across the gap into the valence band, leading to an additional positive charge in the valence band and, correspondingly, to a negative free charge in the conduction band, as shown in Fig. 4. This scattering process is interpreted as the *hole initiated impact ionization*, and due to the above explanations, the corresponding ionization rate can be determined using the very same numerical scheme as in the calculation of the ionization rate of electrons described above. The sole difference is the inversion of the dispersion relation.

The respective impact ionization rates are calculated for holes in all four valence bands. Holes in the upper valence band cannot initiate ionization processes. In GaN and ZnS the main contribution arises from the lowest and second lowest band, whereas in SrS only holes from the lowest valence band are able to initiate ionization events.

TABLE III. Parameters for interpolation formula, Eq. (3), of the energy dependent impact ionization rate for electrons in the wide band gap materials GaN (using band structure *A*), ZnS, and SrS.

Material	E_{th} (eV)	$P(10^{10}\,\mathrm{eV}^{-a}\,\mathrm{s}^{-1})$	a	Remark
GaN	3.7	0.0949	6.434	best fit for $E>6.0$ eV
GaN	3.6	0.00949	7.434	best fit for $E<5.0$ eV
ZnS	3.8	5.935	5.073	
SrS	4.0	59.723	3.182	

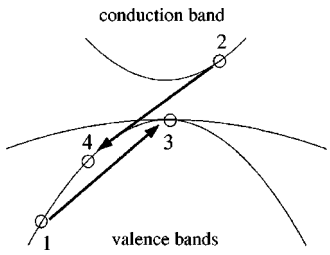

FIG. 4. Schematic impact ionization process of holes (process II).

The wave vector dependent ionization rate $r(\mathbf{k},n)$ is averaged over the Brillouin zone according to Eq. (2), including all four valence bands, which gives the energy dependent ionization rate $R(E)$ shown in Fig. 5 for the three wide band gap materials. Previous theoretical results of Oguzman *et al.*[13] for the threshold region of GaN using the band structure *B* are included for comparison. The shaded area covers their nonaveraged, *k*-dependent rates according to the band structure *B* via $E(k)$. For comparison, the inset shows our nonaveraged, *k*-dependent rates displayed in the same manner using the EPM band structures *A* and *B* (full and open circles). As can be seen, the calculated rate is relatively insensitive to modest changes in the band structure itself. The rates of Oguzman *et al.* are up to two orders of magnitude higher than ours. The reason for this difference is unknown, but could be due to the different integration scheme or screening model used by those authors in the numerical calculations. The corresponding parameters of the simple interpolation formula $\tilde{R}(E)$ according to Eq. (3) are given in Table IV.

Compared with the electron initiated impact ionization rates given in Fig. 3, two special features have to be noticed for the hole rates. First, the threshold energy for hole ionization is in general slightly lower than for electron ionization.[18] This result is due to the flat shape of the top of the upper valence bands, which allows holes to initiate ionization events as soon as they have reached a kinetic energy equal to the gap energy. In the case of SrS, the width of the upper valence band is too narrow to allow holes to gain enough kinetic energy to initiate ionization events due to energy conservation. For this reason, only holes in the lowest valence band contribute to the ionization rate and, therefore, SrS does not show the usual threshold behavior near the gap energy. Instead, the ionization rate sets in only above 14.7 eV and immediately jumps to very high values.

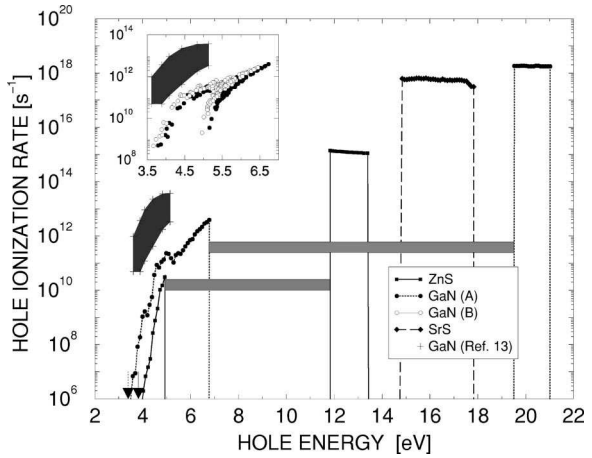

FIG. 5. Energy dependent hole impact ionization rate for the wide band gap materials ZnS, GaN, and SrS. Hole energies are measured from the valence band maximum. The arrows mark the threshold energies. The inset shows a comparison with results of Oguzman *et al.* (see Ref. 13) in more detail (shaded area).

TABLE IV. Parameters for interpolation formula, Eq. (3), of the energy dependent hole ionization rates for GaN (using band structure *A*) and ZnS. Because no ionization events occur for holes in the upper three valence bands of SrS, no interpolation formula can be given for this material.

Material	E_{th} (eV)	$P(10^9\ \mathrm{eV}^{-a}\ \mathrm{s}^{-1})$	a
GaN	3.4	3.5	5.33
ZnS	3.8	7.1	6.23
SrS	...	...	...

The behavior of the hole ionization rate at very high energies should be approximately given by the Born approximation (Bethe formula). The very high density of states in that region leads to a strong suppression of any anisotropy effects induced by the band structure so that the curves are smooth. The high scattering rates calculated at high hole energies arise from the very high density of states in the lower lying valence bands, which lead to physically unrealistic rates. However, no holes in practice can obtain such high energies (unless they are excited by x-ray emission), and therefore this issue is unimportant in device performance.

The second characteristic of the hole impact ionization rates displayed in Fig. 5 is that they vanish in a certain energy range completely, i.e., between about 5 and 12 eV for ZnS and 7 and 19.5 eV for GaN. For higher energies, they set in again immediately as discussed already for SrS. This special behavior is due to the occurrence of an energy gap between the upper three valence bands and the lowest one (compare the band structures, Fig. 2, and Table II), and therefore no states are available for energetic holes.

Thus, the hole initiated impact ionization rate shows a very different behavior compared with the respective electron rate except for the region near the threshold energy, if hole ionization occurs there at all. Since the hole scattering rates are as low as the electron rates near the threshold energy, and vanish completely in the medium energy range, we conclude that hole initiated impact ionization processes can be neglected compared with electron initiated processes in the case of both ZnS and SrS.

IV. IONIZATION COEFFICIENT

The only available data on the impact ionization coefficient for ZnS is based on photocurrent multiplication data obtained by Thompson and Allen[8] in thin Schottky barrier samples. Earlier we compared their extracted impact ionization coefficient data versus field using the results of our previous calculation of the electron impact ionization rate and a full-band ensemble Monte Carlo simulation, using the optical deformation potential as a parameter to fit these data.[5] Thompson and Allen extracted the impact ionization coeffi-

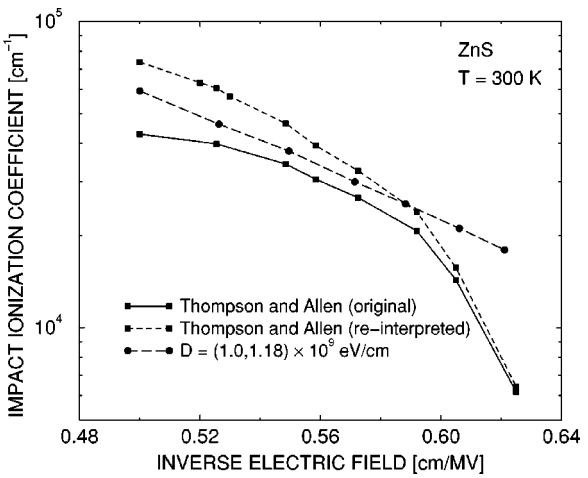

FIG. 6. Comparison of the impact ionization coefficient calculated by Thompson and Allen (see Ref. 8) with the reinterpreted rates assuming electrons only. For comparison, we show Monte Carlo results assuming the deformation potentials shown.

cient from the photocurrent multiplication versus maximum electric field data, assuming the electron and hole ionization coefficients are equal. However, our conclusion from the previous sections is that the hole ionization rate is nearly zero for ZnS, hence $\alpha_p \cong 0$ for all fields. This result has led us to reexamine the interpretation of the impact ionization coefficient for electrons derived from these data.

In order to directly compare the previous results of Thompson and Allen, we have used the same technique employed by those authors based on the method described by Moll[19] to convert multiplication data into a field dependent impact ionization coefficient. For the case in which only electrons are capable of band-to-band impact ionization, the relationship between the electron multiplication M_n and the electron impact ionization coefficient α_n is given by

$$M_n = \exp\left(\int_0^W \alpha_n \, dx \right), \tag{4}$$

where W is the depletion region width. Assuming that the field dependence of the impact ionization coefficient may be expressed by the functional form

$$\alpha_n(E) = \alpha_0 \exp(-b/E), \tag{5}$$

where E is the electric field and b is a parameter, Eq. (4) may be written as

$$\ln M_n(E_{\max}) = \alpha_n(E_{\max}) W_{\text{eff}}, \tag{6}$$

where $E_{\max}$ is the maximum electric field at the surface, and W_{eff} is the effective depletion region width which is given by Moll as W times an integral depending on $E_{\max}$ and b varying between 0 and 1. Through an interative procedure, b is adjusted to achieve the closest fit between the extracted α_n and the model form given by Eq. (5). In the present work we performed this procedure using a least squares algorithm and iterating to find b.

Figure 6 shows a comparison between the original impact ionization coefficient reported by Thompson and Allen, and the reinterpreted rate assuming electron ionization only. Here a best fit to the new data was obtained with $b = 1.31 \times 10^7$ V/cm. As can be observed, the newer result shows less curvature at high fields, reaching a higher value for the coefficient. This provides a slightly better fit to Monte Carlo results reported earlier by us,[5] assuming a particular set of two deformation potential constants for the lowest and upper conduction bands.

It should be noted that the extraction of the impact ionization coefficient from multiplication data in a one-sided step junction is difficult, and may be influenced by gain saturation effects at high fields due to series resistance, junction heating, defects, etc., while at low fields, the experimental determination of M_n is difficult as it is close to unity. Therefore it is difficult to conclude that one method is more ''correct'' than another for extracting the ionization coefficient, or whether the curvature of the experimental data compared to Monte Carlo simulation is real or an artifact.

V. CONCLUSIONS

We have determined the hole initiated impact ionization rates for GaN, ZnS, and SrS. These three wide band gap semiconductors are among the materials currently under intense investigation due to their suitability to serve as active layers for high-field electronic and optoelectronic devices. The electronic properties are described in the framework of the empirical pseudopotential method. The calculation of the hole initiated impact ionization rate follows closely the numerical procedure used for the evaluation of the respective electron rate earlier.

Our main conclusion is that the narrow width of the three upper valence bands prevents hole ionization processes to occur near the gap energy in SrS, while strongly suppressing this process in ZnS. A significant difference compared with the electron rates is due to the second energy gap within the valence bands. This gap represents a forbidden region for the energy of holes, and is therefore responsible for the absence of hole ionization processes within the corresponding energy interval. Thus we conclude that hole ionization is a weak process in such wide band gap semiconductors at high fields, and can be neglected in comparison with the electron impact ionization process.

Based on this assertion, we have reinterpreted the impact ionization coefficient versus field data of Thompson and Allen derived assuming equal electron and hole coefficients, and find a higher impact ionization coefficient for electrons at higher fields, with less curvature in the standard plot versus inverse electric field, which is in qualitative agreement with full-band Monte Carlo simulation results.

ACKNOWLEDGMENTS

The authors would like to thank Peter Vogl at the Walter Schottky Institute, Munich, for his assistance in the band structure calculations. This work was supported by DARPA under the Phosphor Technology Center of Excellence, Grant No. MDA 972-93-1-0030, and by the Deutsche Forschungsgemeinschaft under Grant No. Re 882/6-2.

[1] W. M. Ang, S. S. Pennathur, L. Pham, J. F. Wager, S. M. Goodnick, and A. A. Douglas, J. Appl. Phys. **77**, 2719 (1995).
[2] D. K. Ferry and S. M. Goodnick, *Transport in Nanostructures* (Cambridge University Press, Cambridge, 1997).
[3] M. Stobbe, R. Redmer, and W. Schattke, Phys. Rev. B **49**, 4494 (1994).
[4] M. Reigrotzki, M. Stobbe, R. Redmer, and W. Schattke, Phys. Rev. B **52**, 1456 (1995).
[5] M. Reigrotzki *et al.*, J. Appl. Phys. **80**, 5054 (1996).
[6] M. Dür, S. M. Goodnick, S. S. Pennathur, J. F. Wager, M. Reigrotzki, and R. Redmer, J. Appl. Phys. **83**, 3176 (1998).
[7] M. Reigrotzki, M. Dür, W. Schattke, N. Fitzer, R. Redmer, and S. M. Goodnick, Phys. Status Solidi B **204**, 528 (1997).
[8] T. D. Thompson and J. W. Allen, J. Phys. C **20**, L499 (1987).
[9] N. Sano and A. Yoshii, Phys. Rev. B **45**, 4171 (1992).
[10] Z. H. Levine and S. G. Louie, Phys. Rev. B **25**, 6310 (1982); M. S. Hybertson and S. G. Louie, Phys. Rev. Lett. **55**, 1418 (1985); Phys. Rev. B **34**, 5390 (1986).
[11] H. K. Jung, K. Taniguchi, and C. Hamaguchi, J. Appl. Phys. **79**, 2473 (1996).
[12] M. L. Cohen and J. R. Chelikowsky, *Electronic Structure and Optical Properties of Semiconductors* (Springer, Berlin, 1988).
[13] I. H. Oguzman, E. Bellotti, K. F. Brennan, J. Kolnik, R. Wang, and P. P. Ruden, J. Appl. Phys. **81**, 7827 (1997).
[14] I. H. Oguzman, J. Kolnik, K. F. Brennan, R. Wang, T.-N. Fang, and P. P. Ruden, J. Appl. Phys. **80**, 4429 (1996).
[15] Y. Kaneko and T. Koda, J. Cryst. Growth **86**, 72 (1988).
[16] M. Städele, J. A. Majewski, P. Vogl, and A. Görling, Phys. Rev. Lett. **79**, 2089 (1997).
[17] J. Kolnik, I. H. Oguzman, K. F. Brennan, R. Wang, and P. P. Ruden, J. Appl. Phys. **79**, 8838 (1996).
[18] M. Dür, S. M. Goodnick, R. Redmer, M. Reigrotzki, M. Städele, and P. Vogl, J. Soc. Inf. Dis. (in press).
[19] J. L. Moll, *Physics of Semiconductors* (McGraw–Hill, New York, 1964); J. Cryst. Growth **86**, 72 (1988).